

# **ROCK PROPERTIES INFLUENCING IMPEDANCE SPECTRA STUDIED BY LAB MEASUREMENTS ON POROUS MODEL SYSTEMS**

J. Volkmann<sup>1</sup>, N. Klitzsch<sup>1</sup>, O. Mohnke<sup>1</sup>, and N. Schleifer<sup>2</sup>

<sup>1</sup> Applied Geophysics and Geothermal Energy, E.ON Energy Research Center, RWTH-Aachen, Mathieustr. 10, D - 52074 Aachen, Germany

<sup>2</sup> Wintershall Holding GmbH, Rechterner Straße 2, 49406 Barnstorf, Germany

*This paper was prepared for presentation at the International Symposium of the Society of Core Analysts held in Napa Valley, California,, USA, 16-19 September, 2013*

## **ABSTRACT**

The wetting condition of reservoir rocks is a crucial parameter for the estimation of reservoir characteristics like permeability or residual saturation. Since standard methods are often costly, especially in terms of time, we aim at assessing wettability of reservoir rocks using impedance spectroscopy (IS), a frequency dependent measurement of complex electric resistivity.

IS is sensitive to the electrochemical properties of the inner surface of rocks. These electrochemical properties on the other hand, are decisively influencing wettability. Unfortunately, besides wettability there are other parameters (e.g. pore/grain size) influencing the impedance spectra of rocks. To be able to quantify the relative importance of parameters influencing rock IS response, we study model systems which consist of sintered porous silica beads of different sizes leading to samples with different pore sizes. The main advantage of using model system compared to natural rocks is its well-defined and uniform mineralogical composition and thus uniform electrochemical surface properties.

In order to distinguish pore geometry, fluid electrochemistry and wettability (contact angle) effects on the IS properties we measured the IS response of the fully water saturated model systems in the frequency range from 1 mHz to 1kHz. The influence of wettability was studied by modifying the originally hydrophilic silica beads surface into a hydrophobic state. The wettability change was verified by contact angle measurements. As results, we find pore size dependent relaxation times and salinity dependent chargeabilities for the hydrophilic samples, whereas for the hydrophobic samples chargeabilities are close to zero and independent of pore size and water salinity.

## **INTRODUCTION**

Over the last decade significant progress has been made in the understanding of the mechanisms causing frequency dependent electrical impedances measured by Impedance Spectroscopy (IS), in geophysics also known as Spectral Induced Polarization (SIP). However, integrated models involving different polarization processes at the micro-scale

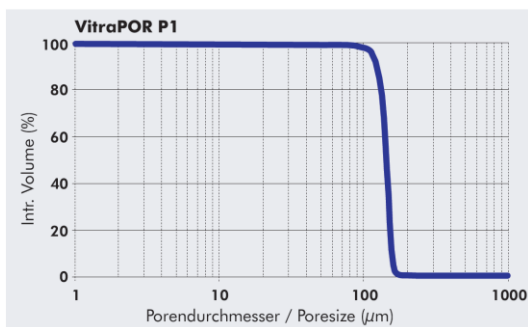
are still missing, in particular with respect to the wetting condition of the inner rock surface. Moreover, the large number of rock parameters influencing the impedance spectra, often not exactly known for natural rock samples, hinders finding a universal relation between IS and wettability heuristically. Therefore, we use a model system of sintered porous silica beads to quantify the influencing parameters, improve the understanding of the underlying mechanisms and thereby uncover solely wetting related influences on IS.

## SAMPLES

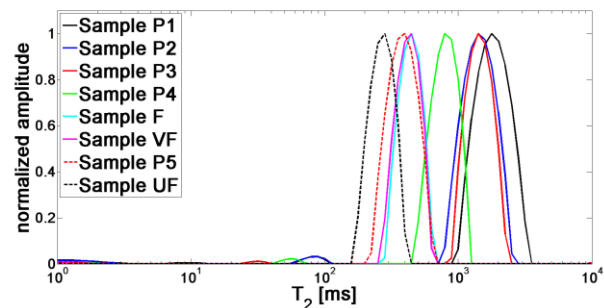
For our studies, we use eight custom made cylindrical samples with 2 cm in diameter and 3 cm in height (+ additional samples for reproducibility tests). These are sintered porous ceramics, manufactured by ROBU® Sintered Glassfilters [1], of pure borosilicate 3.3 standard glass according to ISO 4793 and DIN/ISO 3585. Main advantage is their well-known chemical composition and narrow pore size distribution (Figure 1), as well as the available material characterization by the manufacturer. The unimodal pore size distribution is confirmed by NMR relaxometry measurements (Figure 2) with the transversal relaxation time  $T_2$  as a measure of pore size:  $T_2 \sim \text{pore size}$  [2].

In the current study, we obtained additional porosity information by weighing of the dry and saturated samples and by NMR relaxometry. Scanning electron microscopy (SEM) images were taken to get a better idea of the pore space geometry (Figure 3).

The samples were brought to a hydrophobic state by Cobra Technologies B.V. [3] in cooperation with Ergotech Ltd [4] by means of a hydrophobic agent attached to the inner surface of the samples. Some of the samples were cut after hydrophobization and contact angles were measured on water drops on the cut inner surface (Table 1). This procedure was impossible in original state due to immediate spontaneous imbibition, which at the same time shows their hydrophilic character. A typical sample after hydrophobization is shown in Figure 4.



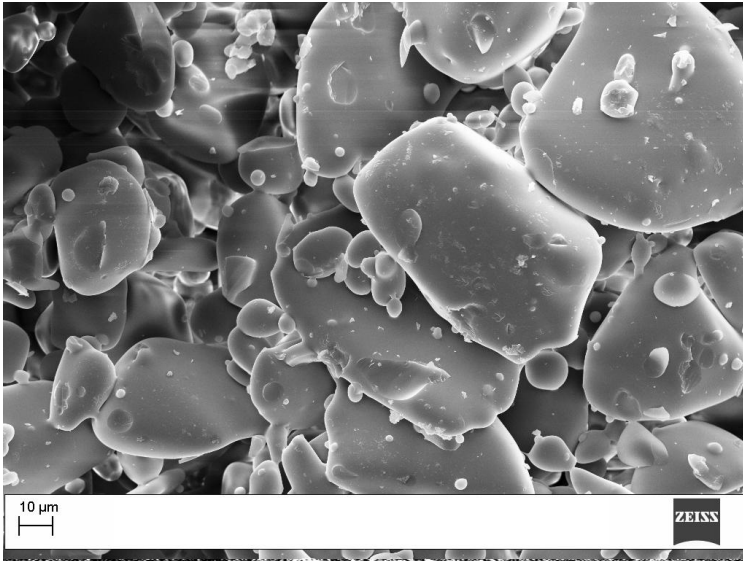
**Figure 1:** Exemplary cumulative pore size distribution of sample P1 as given by ROBU® Glasfilter-Geräte GmbH.



**Figure 2:** NMR  $T_2$  distributions of hydrophilic porous borosilicate samples of different pore sizes (Table 1) confirm their narrow and unimodal pore size distribution.

**Table 1:** Pore diameter  $d_{por}$ , porosity  $\phi$ , specific surface area  $S_{por}$  (BET) and contact angle  $\theta_{hydrophobic}$  (after hydrophobization).

Sample ID	$d_{por} / \mu\text{m}$	$\phi$	$S_{por} / \text{m}^2\text{g}^{-1}$	$\theta_{hydrophobic} / ^\circ$
P1	100 – 160	32%	0.085	-
P2	40 – 100	30%	0.130	115.1
P3	16 – 40	44%	0.350	-
P4	10 – 16	39%	0.500	-
F <sub>1</sub> , F <sub>2</sub>	4 – 5.5	51%, 53%	1.200	125.1, -
VF <sub>1</sub> , VF <sub>2</sub>	2 – 2.5	46%, 41%	N/A	124.8, -
P5	1.0 – 1.6	54%	1.750	-
UF <sub>1</sub> , UF <sub>2</sub> , UF <sub>3</sub>	0.9 – 1.4	46%, 48%, 51%	1.750	127.4, -, -

**Figure 3:** Scanning electron microscopy (SEM) image of sample P4 [5].**Figure 4:** Porous borosilicate sample (diameter: 2 cm, height: 3 cm) with water drops on hydrophobic inner surface.

## METHODS

We introduce Impedance Spectroscopy (IS) measurements, i.e. frequency dependent complex resistivity/conductivity measurements, in the frequency range from 1 mHz to 1 kHz using a four-electrode setup together with the ZEL-SIP04 instrument [6]. The following IS parameters are studied:

1. The influence of pore radii by using 8 different sample types with nominal pore sizes  $d_{por}$  between 0.9  $\mu\text{m}$  and 160  $\mu\text{m}$ , see Table 1.
2. The influence of fluid salinity with NaCl solutions in a conductivity ( $\sigma_{fluid}$ ) range between  $2 \cdot 10^{-4} \text{ S m}^{-1}$  and  $5 \cdot 10^{-2} \text{ S m}^{-1}$ .
3. The influence of wettability by application of a hydrophobic agent to the inner glass surfaces for 4 selected samples (P2, F, VF, UF, see Table 1).

Subsequently, we analyze the IS spectra using a Cole-Cole model for the dependence of the electrical resistivity  $\rho$  on angular frequency  $\omega$ .

$$\rho(\omega) = \rho_0 \left[ 1 - m \left( 1 - \frac{1}{1 - (i\omega\tau)^c} \right) \right] \quad (1)$$

with DC – resistivity  $\rho_0$ , chargeability  $m$ , frequency exponent  $c$  and relaxation time  $\tau$ .

## RESULTS

IS results for the frequency range 10 mHz to 200 Hz are presented in Figure 5 to Figure 10. Regarding the influence of fluid conductivity, we find a general trend of decreasing phase peak values with fluid conductivity (Figure 5). In terms of chargeability (see equation 1), this is in agreement with previous results [7,8]. Regarding the influence of wettability, we find decreasing phase values with increasing contact angles (Figure 6). In particular, the low frequency data do not show a distinct phase maximum for the hydrophobic samples. This observation can be explained by a disturbance of the surface-fluid interaction being responsible for considerable phase effects (e.g. [9]) due to the water repellent surface. Unfortunately, this fact prevents us from applying a quantitative analysis of hydrophobic data in terms of Cole-Cole parameters. Additionally, the phase maxima decrease with increasing pore sizes (Figure 7). A summary of the maximum phase values below 100 Hz for hydrophilic and hydrophobic samples as a function of fluid salinity and pore sizes is given in Figure 9 and Figure 10. It shows the decrease of the phase values with pore size, salinity and contact angle. For hydrophilic samples, a corresponding behavior can be found in terms of chargeability (not shown).

The corresponding peak frequencies are correlated to increasing pore sizes (Figure 7). This is in qualitative agreement with the wide range of (e.g. Cole-Cole) relaxation times found in previous studies [8,10,11,12,13,14]. A quantitative analysis, assuming a power law relationship for the hydrophilic samples (Figure 8), leads to dependence  $\tau \sim d_{\text{por}}^{1.3 \pm 0.2}$  of relaxation time  $\tau$  on nominal pore size  $d_{\text{por}}$  considering all salinities. Considering the different salinities separately, the exponent is in a range of 1.0 to 1.9, thus it is in the range of earlier results yielding exponents between 1 and 3 [12,13,14]., whereas theory usually proposes an exponent of 2 [15,16,17].

## CONCLUSIONS AND OUTLOOK

IS properties of an experimental reference system of porous borosilicate samples have been studied and compared to results on natural rock systems. We can reproduce published experimental results regarding decreasing phase shifts with increasing fluid salinity and with increasing pore sizes in the low frequency range below 1 kHz. Furthermore, we find a quantitative relation between Cole-Cole relaxation time and pore size which is in agreement with previous data. With respect to wettability, it is possible to distinguish between water wet and oil wet sample state from noticeably higher maximum phase values of the water wet samples. Unfortunately, water wet and oil wet rocks can only be distinguished in case of sufficiently low pore sizes and fluid salinities, i.e. not for the high salinity brines typically found in reservoirs.

In a next step, we will apply our reference system results to test recently proposed relations between electrical properties and macroscopic rock properties like inner surface

or permeability. Furthermore, a wider frequency range (up to 10 MHz) will be analyzed in terms of a wideband data interpretation scheme to capture information from different often overlapping polarization processes.

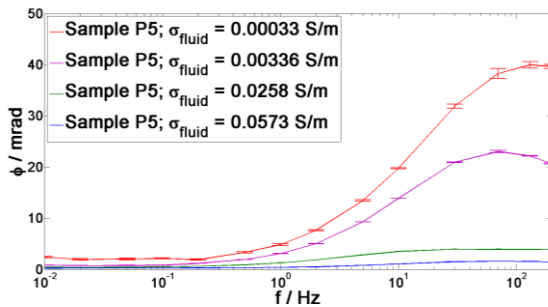


**Figure 5:** Examples of phase spectra (hydrophilic samples). Phase maximum decreases with increasing fluid conductivity  $\sigma_{\text{fluid}}$  at fluid temperatures between 18.3°C and 19.8°C.

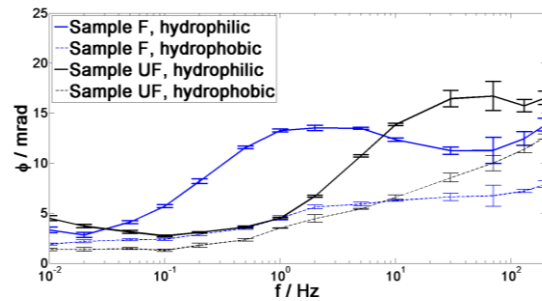


**Figure 6:** Examples of phase spectra at  $\sigma_{\text{fluid}} \approx 2 \cdot 10^{-4} \text{ S m}^{-1}$ . Phase maximum decreases with increasing wetting angle  $\theta$ .

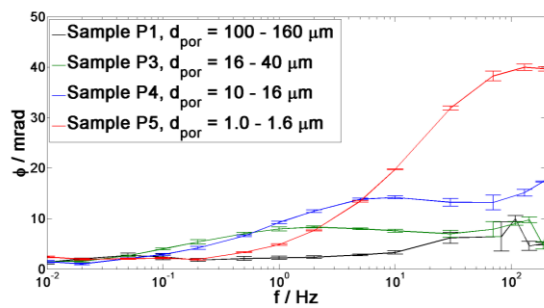


**Figure 7:** Examples of phase spectra (hydrophilic samples at  $\sigma_{\text{fluid}} \approx 3 \cdot 10^{-4} \text{ S m}^{-1}$ ). The amplitude of the phase maximum and the position of the corresponding peak frequency both decrease with increasing pore size  $d_{\text{por}}$ .

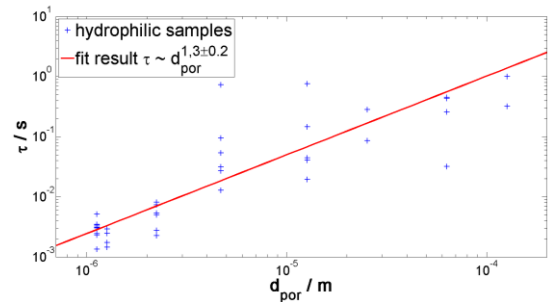


**Figure 8:** Dependence of Cole-Cole relaxation time  $\tau$  on pore diameter  $d_{\text{por}}$  for hydrophilic samples. A dependence of  $\tau \sim d_{\text{por}}^{1.3 \pm 0.2}$  on nominal pore size is found.

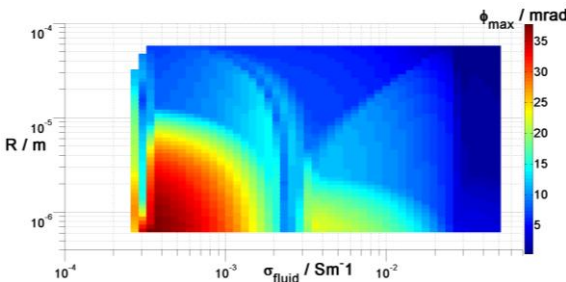


**Figure 9:** Maximum phase  $\phi_{\text{max}}$  below 100 Hz for hydrophilic samples as a function of fluid conductivity  $\sigma_{\text{fluid}}$  and pore radius  $R$ .

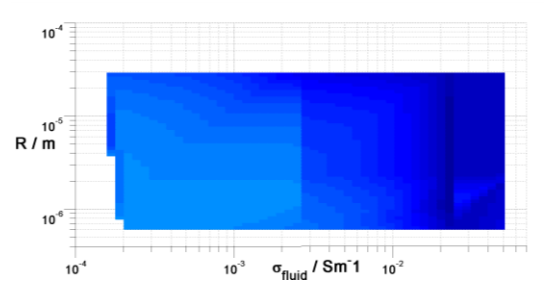


**Figure 10:** Maximum phase  $\phi_{\text{max}}$  below 100 Hz for hydrophobic samples as a function of fluid conductivity  $\sigma_{\text{fluid}}$  and pore radius  $R$ .

## ACKNOWLEDGEMENTS

The presented study is supported by the Deutsche Wissenschaftliche Gesellschaft für Erdöl, Erdgas und Kohle e.V. (DGMK) - in particular by its members ExxonMobil Production Deutschland GmbH, GDF SUEZ E&P Deutschland GmbH, RWE Dea AG and Wintershall Holding GmbH - in the framework of the DGMK project 703 “IS for assessing the wetting conditions of reservoir rocks” and by the Collaborative Research Center TR32 of the German Research Foundation (DFG). Furthermore, the authors thank L. Ahrensmeier, M. Penz and T. Houben for their assistance during laboratory work.

## REFERENCES

1. Robu@ Glasfilter-Geräte GmbH, Schützenstraße 13, D - 57644 Hattert, Germany.
2. Brownstein, K.R., Tarr, C.E., 1979, “Importance of classical diffusion in NMR studies of water in biological Cells”, *Phys. Rev. A* 19 (1979), 2446.
3. Cobra Technologies B.V., Rondweg 48, 7468 MC ENTER, The Netherlands.
4. ErgoTech Ltd, Unit 3 Cae Ffwyt Business Park, Glan Conwy, Conwy, LL28 5SP, UK
5. Wiens, E., *NMR and SIP properties of partially saturated porous silica glasses* (Diploma thesis), RWTH-Aachen University, Aachen, Germany, (2009).
6. Zimmermann, E., *Phasengenaue Impedanzspektroskopie und –tomographie für geophysikalische Anwendungen (PhD-Thesis)*, Rheinische Friedrich-Wilhelms-Universität Bonn, Bonn, Germany, (2010).
7. Lesmes, D.P., Frye, K.M., “Influence of pore fluid chemistry on the complex conductivity and induced polarization responses of Berea sandstone”, *Journal of Geophysical Research*, (2001) **106**, B3, 4079–4090.
8. Titov, K., Tarasov, A., Yuri, I., Seleznev, N., Boyd, A., “Relationships between induced polarization relaxation time and hydraulic properties of sandstone”, *Geophysical Journal International*, (2010) **180**, 1095–1106.
9. Chelidze, T., Guegen, Y., “Electrical spectroscopy of porous rocks: a review-I. Theoretical models”, *Geophysical Journal International* (1999), **137**, 1-15
10. Scott, J.B.T., Barker, R.D., “Determining pore-throat size in Permo-Triassic sandstones from low-frequency electrical spectroscopy”, *Geophysical Research Letters*, (2003) **30**, 9, 1450.
11. Scott, J.B.T., Barker, R.D., “Characterization of sandstone by electrical spectroscopy for stratigraphical and hydrogeological investigations”, *Quarterly Journal of Engineering Geology and Hydrogeology*, (2005) **38**, 143–154.
12. Binley, A., Slater, L.D., Fukes, M., Cassiani, G., “Relationship between spectral induced polarization and hydraulic properties of saturated and unsaturated sandstone”, *Water Resources Research*, (2005) **41**, W12417.
13. Kruschwitz, S., *Assessment of the complex resistivity behavior of salt affected building materials* (Ph.D.-thesis), Fakultät VI - Planen Bauen Umwelt der Technischen Universität Berlin, Berlin, Germany (2007).
14. Kruschwitz, S., Binley, A., Lesmes, D., Elshenawy, A., “Textural controls on low frequency electrical spectra of porous media”, *Geophysics*, (2010) **75**, 4, WA113–WA123.
15. Marshall, D.J., Madden, T.K., “Induced polarization, a study of its causes”, *Geophysics*, (1959) **24**, 4, 790–816.
16. Titov, K., Komarov, V., Tarasov, V., Levitski, A. “Theoretical and experimental study of time domain-induced polarization in water-saturated sands”, *Journal of Applied Geophysics*, (2002) **50**, 417–433.
17. Revil, A., Florsch, N., “Determination of permeability from spectral induced polarization in granular media”, *Geophysical Journal International*, (2010) **181**, 1480–1498.